Original Article

MOLECULAR METABOLISM

Circadian clock network desynchrony promotes weight gain and alters glucose homeostasis in mice

Isa Kolbe [1], Brinja Leinweber [1], Matthias Brandenburger [2], Henrik Oster [1,*]

ABSTRACT

Objective: A network of endogenous circadian clocks adapts physiology and behavior to recurring changes in environmental demands across the 24-hour day cycle. Circadian disruption promotes weight gain and type 2 diabetes development. In this study, we aim to dissect the roles of different tissue clocks in the regulation of energy metabolism.

Methods: We used mice with genetically ablated clock function in the circadian pacemaker of the suprachiasmatic nucleus (SCN) under different light and feeding conditions to study peripheral clock resetting and the role of the peripheral clock network in the regulation of glucose handling and metabolic homeostasis.

Results: In SCN clock-deficient mice, behavioral and non-SCN tissue clock rhythms are sustained under rhythmic lighting conditions but deteriorate quickly in constant darkness. In parallel to the loss of behavioral and molecular rhythms, the animals develop adiposity and impaired glucose utilization in constant darkness. Restoring peripheral clock rhythmicity and synchrony by time-restricted feeding normalizes body weight and glucose metabolism.

Conclusions: These data reveal the importance of an overall synchronized circadian clockwork for the maintenance of metabolic homeostasis.

Keywords Body weight; Constant darkness; Suprachiasmatic nucleus; Circadian clock; Glucose metabolism; Light-dark cycle

1. INTRODUCTION

In most species, including humans, a network of endogenous so called circadian clocks coordinates molecular, physiological, and behavioral 24-hour rhythms, adapting the organism to recurring changes in environmental conditions brought about by the rotation of the Earth around its axis. At the molecular level, circadian cellular oscillators are based on an interlocked system of transcriptional-translational feedback loops (TTFLs). In the central TTFL, the transcription factors brain and muscle ARNT-like 1 (BMAL1) and circadian locomotor output cycles kaput (CLOCK) activate transcription of three period (*Per1-3*) and two cryptochrome (*Cry1-2*) genes during the day. In the night, PER/CRY protein complexes accumulate in the nucleus and interfere with CLOCK/BMAL1 action, thus suppressing their own transcription. Towards the next morning, PER/CRY protein complexes become degraded and thereby relieve CLOCK/BMAL1 suppression [1].

In complex organisms such as mammals, circadian energy metabolism is orchestrated by an interplay of central and peripheral clocks, with a master pacemaker being located in the suprachiasmatic nucleus (SCN) and subordinate clocks in non-SCN central and peripheral tissues [2]. Under rhythmic light-dark (LD) conditions the SCN is entrained to the external light cycle and passes this temporal information on to temporally coordinate the circadian tissue oscillator network [3]. Clock gene/protein oscillations are conveyed into physiological functions through rhythmically regulated tissue-specific clock-output genes (CCGs), resulting in marked daily variations of rest/activity, feeding/fasting and oscillating levels of various metabolic parameters [4–6]. Not only do baseline blood levels of glucose and insulin oscillate but also beta cell insulin responses and target tissue insulin sensitivity show marked variations over the course of the day [7,8].

Disruptions of the circadian timing network — as seen in human shift workers or through genetic modifications of circadian clock genes — alter metabolic setpoints and promote the development of metabolic disorders including obesity and impaired glucose utilization [9,10]. In mice, disruption of the essential clock gene *Bmal1* is accompanied by arrhythmic behavior and various metabolic dysregulations. While Bmal1 KO mice are overall small and lean, they show high levels of ectopic lipid deposits in liver and muscle, glucose intolerance, and overall low insulin levels [11–14]. *Clock* mutant mice, on the other hand, are obese and hyperphagic with hyperlipidemia and hyperglycemia and develop metabolic syndrome under high-fat diet conditions [15]. In whole-body clock mutants it is difficult to distinguish the impact of different tissue oscillators on metabolic regulation. Animals with a surgically removed SCN, however, develop a pre-diabetic,

[1]Institute of Neurobiology, University of Lübeck, Lübeck, Germany [2]Fraunhofer Research Institution for Marine Biotechnology and Cell Technology, Lübeck, Germany

*Corresponding author. E-mail: henrik.oster@uni-luebeck.de (H. Oster).

Received April 14, 2019 • Revision received September 23, 2019 • Accepted September 28, 2019 • Available online 8 October 2019

https://doi.org/10.1016/j.molmet.2019.09.012

hyperinsulinemic phenotype with elevated adipose tissue mass suggesting a prominent function of the SCN pacemaker in this context [16]. At the same time, a potential role of peripheral clock function in metabolic regulation is suggested by targeted clock gene manipulation in liver [12,17], pancreatic beta cells [7,8], muscle [18], or adipose tissues [19].

Recent work on genetic models of SCN clock ablation have shown that peripheral clocks align with synchronizers, or *Zeitgebers,* such as food intake independent of pacemaker function pointing at a federated model of circadian network organization and regulation of circadian physiological output [20]. In this paper, we use SCN pacemaker knockout mice to dissect the role of central and peripheral clock function in metabolic homeostasis.

2. METHODS

2.1. Animals

All animal experiments were conducted in accordance with the German law of animal welfare and ethically assessed and licensed by the Ministry of Agriculture, Environment and Rural Areas (MELUR) of the state of Schleswig-Holstein. 10-week old, male *Syt10*$^{Cre/Cre}$ x *Bmal1*$^{flx/-}$ (SCN-enriched deletion of *Bmal1*; SCN-BKO) mice and their control littermates (*Syt10*$^{Cre/Cre}$ x *Bmal1*$^{+/-}$ (Con)) on a C57BL/6 J background were used for all experiments [21]. This Cre-driver is densely expressed throughout the SCN region and leads to an efficient reduction of BMAL1-positive cells in this tissue. Additionally, it can be found dispersed in other CNS sites but is not expressed in non-neuronal tissue with exception of the testis. To increase the SCN *Bmal1*/BMAL1 reduction and the circadian phenotype, mice carried an additional heterozygous *Bmal1* deletion allele. In control mice the heterozygous wildtype allele was sufficient to restore circadian wildtype-like behavior [21]. Mice were single-housed in constant temperature (23 °C) and humidity (55–60%) conditions under a 12:12 h light-dark cycle or constant darkness (DD) with water and chow (Altromin, Lage, Germany) *ad libitum*, if not stated otherwise. For long-term weight development data, mice and food were weighed in 3-day intervals. Wheel-running activity was recorded and evaluated with ClockLab software (Actimetrics, Austin St. Evanston, USA).

2.2. Food intake, restricted feeding, glucose and insulin tolerance tests

Food was weighed in 6-h intervals over two days in light-dark or constant darkness conditions for short-term profiles. During restricted feeding in constant darkness (DD-RF) conditions mice had access to chow during the initial dark period of their light-dark entrainment phase (*i.e.* 6:00 in the morning to 18:00 in the evening). For the tolerance tests animals were fasted for 12 (glucose) or 4 (insulin) hours and the initial blood values were measured with a glucometer (Accu-Chek Aviva, Roche, Basel, Switzerland). Subsequently, glucose (1.5 g/kg) or insulin (1U/kg) were i.p.-injected and blood glucose levels measured from the tail vein at 15, 30, 60, 90, and 120 min after administration.

2.3. Oxygen consumption, respiratory ratio, and body temperature measurement

Oxygen consumption and carbon dioxide production for respiratory exchange ratio (RER) determination were investigated in an open-circuit indirect calorimetry system (TSE Systems, Bad Homburg, Germany) with data collection in 10-min intervals. Mice were allowed to acclimatize to the system for three days and then oxygen consumption was measured for two days in light-dark followed by three days in constant darkness conditions with the last two days of constant darkness used for analysis. Body weight was measured daily and oxygen consumption normalized to the individual body weight. For temperature measurement, E-mitters (Starr Life Sciences, Oakmont, USA) were transplanted to the abdomen 10 days prior to experiment. Core body temperature was recorded in 1-min intervals with the Vital View (Starr Life Sciences) software for 1 week in light-dark and 3 days in constant darkness while the last 2 days in light-dark and constant darkness were used for analysis. In constant darkness, time intervals were corrected for the shift in activity onsets of control animals with average onset time defined as CT 12. Water and food were provided *ad libitum* throughout both experiments.

2.4. Quantitative real-time PCR (qPCR)

Animals were sacrificed at indicated *Zeitgeber* (ZT; ZT0 = "lights on") or circadian times (CT; CT12 = activity onset in control animals) by cervical dislocation. Liver, pancreas, and epididymal white adipose tissue (eWAT) were dissected, snap-frozen in liquid nitrogen, and stored at −80 °C. TRIzol (Invitrogen, Carlsbad, USA) isolated total RNA was transcribed into cDNA with MultiScribe Reverse Transcription Kit (Applied Biosystems, Foster City, USA) and gene expression determined using iQ-SYBR Green Supermix and a CFX96 thermocycler (Bio-Rad, Hercules, USA). Relative expression values of clock genes and metabolism-associated genes were obtained by ΔΔCT normalization against a house keeping gene, eukaryotic elongation factor 1 alpha (*Eef1α*), which displayed constant and high expression in all analyzed tissues at all measured time points and was used in earlier publications [21]. Primer sequences are available upon request.

2.5. Serum assays

Serum samples were prepared from trunk blood of animals sacrificed at 4 timepoints as indicated above. Serum was transferred after clotting and metabolites and hormones measured by ELISA according to the manufacturers' protocols using the following kits: insulin (Mercodia, Uppsala, SE; Cat # 10-1247-01); leptin (Crystal Chem, Downers Grove, IL; Cat # 90030); glucagon (Mercodia; Cat # 10-1281-01); free fatty acids (Zen-Bio, Research Triangle Park, NC; Cat # SFA-1); triglycerides (Merck, Darmstadt, DE; Cat # TR0100). Glucose was measured using the Accu-Chek monitor (Roche Diagnostics, Mannheim, DE).

2.6. Magnetic resonance imaging (MRI)

For quantification of adipose tissue mass and location, animals were sacrificed by cervical dislocation and measured in a small animal magnetic resonance imaging (MRI) scanner (Aspect Imaging, Hevel Modi'in, Israel) with T1-weighted settings (TE/TR = 10/322.434, FOV = 60 × 30 mm, 21 slices of 1 mm). Regions of interest (ROIs) of subcutaneous and visceral white adipose tissue were manually marked in every slide and the tissue volume interpolated by using the AspectImaging quantification software (Aspect Imaging).

2.7. Statistical analysis

All data are expressed as means ± SEMs. For χ^2 periodogram or Pearson's χ^2 test analysis, we used Clocklab (Actimetrics) and for other statistical comparisons Graph Pad Prism software (GraphPad, La Jolla, USA), with Student's t-tests for one-to-one comparisons, one-way ANOVAs for more than two groups and two-way ANOVAs with Bonferroni post-test for time and group interactions. For all tests, p-values < 0.05 were considered significant. CircWave was used for rhythms analyses of qPCR data.

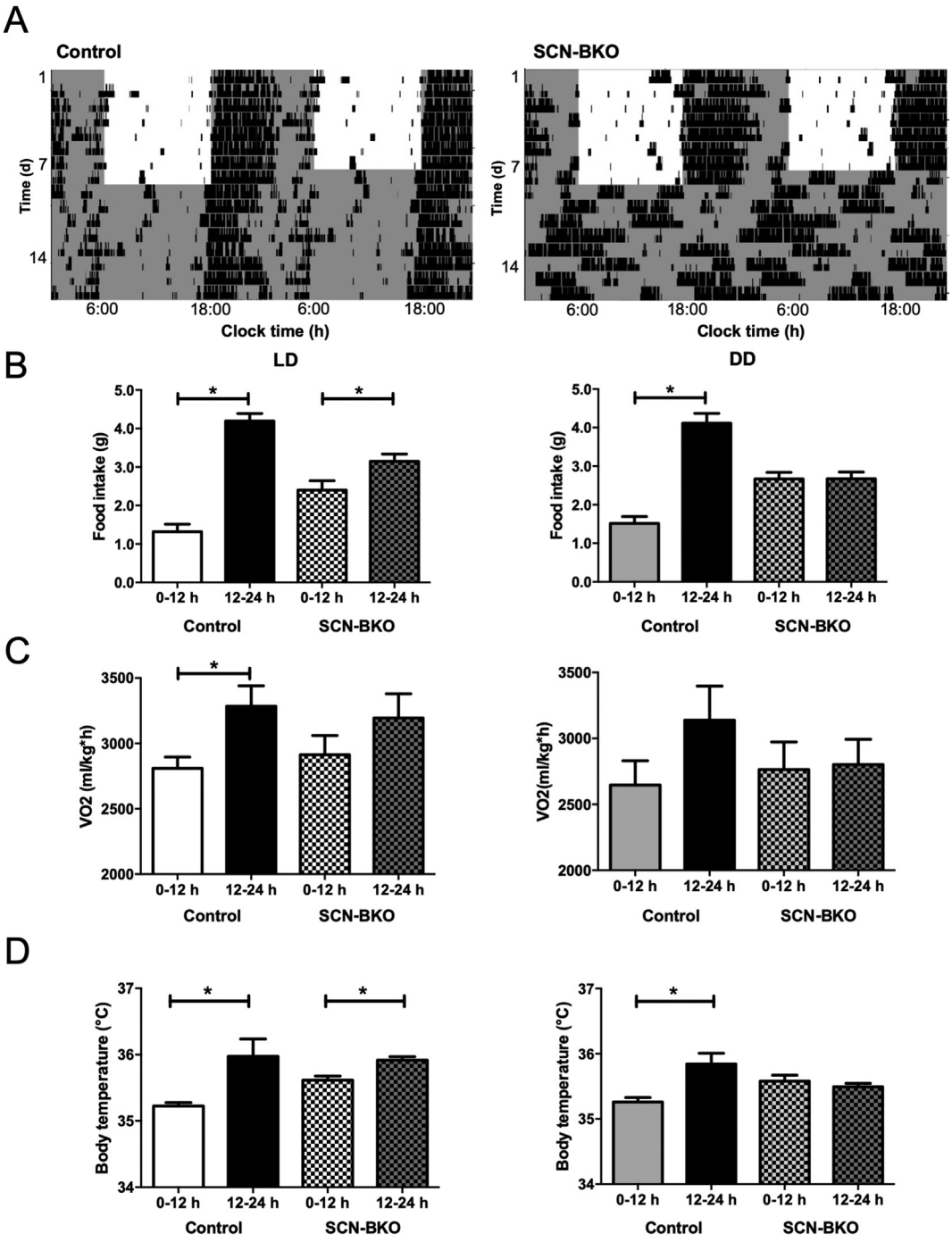

Figure 1: SCN-BKO mice retain behavioral rhythms under light-dark but not under constant darkness conditions. A) Representative actograms of control (left) and SCN-BKO animals (right) under 12-h:12-h light-dark (LD) and constant darkness (DD) conditions. Light phases are indicated by white, dark phases by grey background. B) Day/night food intake profiles of control and SCN-BKO mice in light-dark (left; ANOVA: interaction: $p < 0.001$; time: $p < 0.001$; genotype: $p = 0.933$) and constant darkness (right; ANOVA: interaction: $p < 0.001$; time: $p < 0.001$; genotype: $p = 0.476$). C) Day/night oxygen consumption per hour normalized to body individual body weight of control and SCN-BKO mice in light-dark (left; ANOVA: interaction: $p < 0.525$; time: $p < 0.026$; genotype: $p = 0.967$) and constant darkness (right ANOVA: interaction: $p < 0.312$; time: $p < 0.241$; genotype: $p = 0.621$). D) Day/night core body temperature of control and SCN-BKO mice in light-dark (left; ANOVA: interaction: $p < 0.135$; time: $p < 0.003$; genotype: $p = 0.257$) and constant darkness conditions (right; ANOVA: interaction: $p < 0.007$; time: $p < 0.033$; genotype: $p = 0.878$). Averages ±SEM; $n = 5–6$ animals per condition and genotype; *: $p < 0.05$, 2-way ANOVA with Bonferroni post-test.

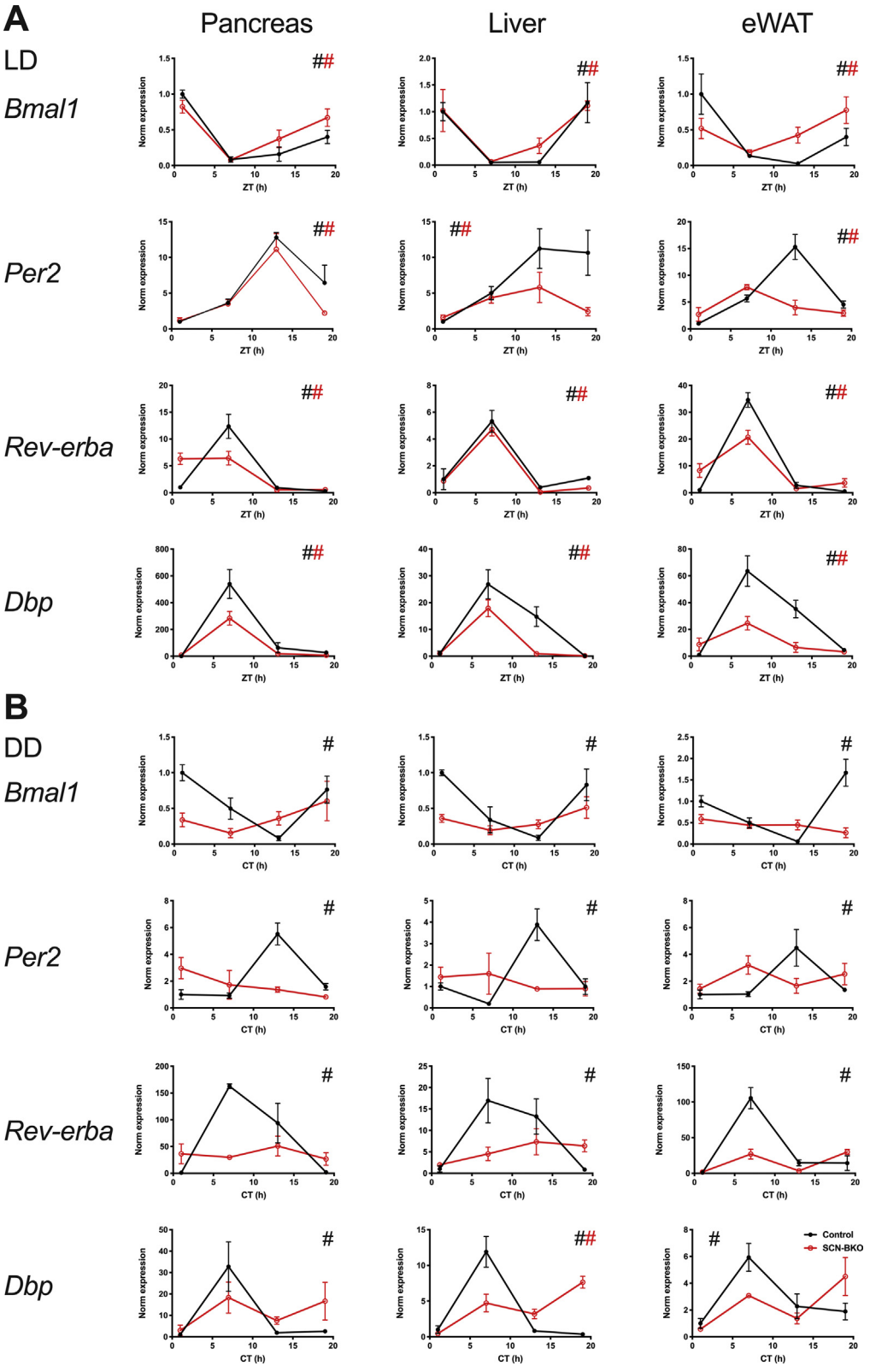

Figure 2: SCN-BKO mice retain molecular clock gene rhythms in peripheral tissues under light-dark, but not under constant darkness conditions. A) mRNA expression profiles of *Bmal1, Per2, Dbp and RevErbα (Nr1d1)* at four time points (*Zeitgeber* time (ZT) 1 = 1 h after "lights on") under light-dark conditions in control (black) and SCN-BKO animals (red) in pancreas, liver, and epididymal white adipose tissue. B) mRNA expression of *Bmal, Per2, Dbp*, and *RevErbα* at four time points (circadian time (CT) 1 = 37 h after "lights off") under constant darkness conditions in control and SCN-BKO animals in pancreas, liver and epididymal white adipose tissue (n = 3–5 animals per time point and genotype, #: rhythmic gene expression, $p < 0.05$, CircWave analysis).

3. RESULTS

3.1. In the absence of a functional SCN clock, behavioral and molecular clock rhythms depend on a regular light-dark cycle

In a standard 12:12 h light-dark cycle, SCN pacemaker function was dispensable for rhythmic running-wheel behavior with both control and SCN-BKO mice displaying a robust 24-hour period of locomotor activity with activity predominantly confined to the dark phase (Figure 1A). In constant darkness conditions, however, SCN-BKO mice immediately and completely lost circadian rest/activity rhythms, while control animals sustained rhythmic activity behavior with an average period of 23.8 ± 0.1 h (Figure 1A). In line with this, in light-dark conditions more food was consumed during the dark in control ($p < 0.0001$) as well as in SCN-BKO ($p = 0.0186$) mice, although day/night variations were dampened in SCN-BKO animals compared to control littermates (Figure 1B, left panel). In constant darkness, already on the second day SCN-BKO animals consumed equal amounts of chow during both halves of the day while, in control animals, circadian food intake rhythms were preserved ($p < 0.0001$; Figure 1B right panel). Although the timing of food intake differed between genotypes, the total daily amount of consumed food was comparable ($p = 0.6841$). Similar to food intake, oxygen consumption was reduced during the inactive light compared to the dark phase (controls: $p = 0.0370$) with a blunted day-night difference ($p = 0.2814$) in SCN-BKO animals (Figure 1C, right panel and Suppl. Fig. 1A, left panel). In constant darkness, in control animals, the difference in oxygen consumption between active and inactive hours was dampened ($p = 0.1732$) and day-to-night differences were lost in SCN-BKO ($p = 0.8971$) mice (Figure 1C, right panel and Suppl. Fig. 1B, left panel). Similarly, daily rhythms in the respiratory exchange ratio (RER) were dampened in SCN-BKO animals in light-dark conditions (Suppl. Fig. 1A, right panel) and lost in constant darkness (Suppl. Fig. 1B, right panel). In light-dark conditions, control ($p = 0.0309$) and SCN-BKO ($p = 0.0104$) mice displayed a lower core body temperature during the light compared to the dark phase (Figure 1D, left panel). In constant darkness conditions, controls diurnal differences were maintained in controls ($p = 0.0167$), while body temperature in SCN-BKOs lost its rhythmicity ($p = 0.4311$; Figure 1D, right panel).

We next used qPCR analysis to assess clock function in metabolically active peripheral tissues under light-dark and constant darkness conditions in SCN-BKO and control mice. In line with the results for behavior, diurnal regulation of peripheral clock gene transcription was observed under light-dark conditions independent of SCN pacemaker function (Figure 2A; $p < 0.05$ for all genes and genotypes). Again — and mimicking what we observed for food intake rhythms — temporal differences were blunted in tissues of SCN-BKO animals indicating rhythm dampening or phase-shift as previously observed [22]. After one week in constant darkness, time-of-day effects in clock gene expression were conserved in control animals ($p < 0.05$ for all genes and tissues), while in SCN-BKO mice, temporal differences were no longer measurable for clock transcripts in any tissue (Figure 2B; $p > 0.05$ for all genes and tissues). Together, these data suggest that SCN pacemaker function is dispensable for rhythmic behavior and tissue clock gene expression in light-dark conditions, while in constant environmental conditions, the SCN pacemaker becomes essential to coordinate coherent rhythms across the organism.

3.2. In the absence of a functional SCN clock, metabolic homeostasis depends on a regular light-dark cycle

We next studied how the regulation of behavioral and molecular clock rhythms under light-dark and constant darkness conditions affected metabolic homeostasis in the absence of a functional SCN clock. Under light-dark conditions, rhythmic expression of metabolically relevant genes previously reported as clock-controlled [23] was retained in all three tissues ($p < 0.05$ for all genes and tissues, except for *Pepck1*). However, expression rhythms for *Acat1* (acetyl-CoA acetyltransferase 1) in pancreas and *Pepck1* (phosphenolpyruvate carboxykinase 1) in liver were markedly dampened (Figure 3A). In contrast, in constant darkness, expression rhythms were completely lost for all genes and tissues in SCN-BKO mice ($p > 0.05$ for all genes and tissues) while little effects of light conditions were seen for control mice (Figure 3B; $p < 0.05$ for all genes and tissues).

Under light-dark conditions, over the course of 10 weeks body weight development and food intake (Figure 3A) were comparable between control and SCN-BKO animals under, both, normal chow (NC) and high-fat diet conditions (Figure 4A and Suppl. Fig 2A). At the end of the experiment, mice were sacrificed and analyzed for body composition by MRI. In line with body weight, adiposity and fat distribution were comparable between both genotypes under both diet conditions (Suppl. Fig. 2B, C; $p > 0.05$ for both depots and diet conditions). In constant darkness conditions, however, SCN-BKO animal gained significantly more weight than their control littermates despite comparable food intake (Figure 4B). Body composition analysis (Figure 4C) at the end of the experiment revealed increased adipose tissue mass for subcutaneous ($p = 0.0409$) and visceral ($p = 0.0252$) white adipose depots in SCN-BKO mice in constant darkness (Figure 4C).

In line with the loss of rhythmic clock and metabolic gene expression in constant conditions we also observed changes in blood metabolic parameters in SCN-BKO mice compared to controls. While under light-dark conditions, serum levels for glucose, insulin, glucagon, leptin, free fatty acids, and triglycerides did not differ significantly between both genotypes ($p > 0.05$ for all parameters), we measured decreased free fatty acid ($p < 0.0001$) and increased glucose ($p = 0.0395$), leptin ($p = 0.0437$), and triglyceride levels ($p = 0.0304$) in SCN-BKO mice under constant darkness conditions (Table 1).

To further evaluate the metabolic ramifications of peripheral circadian desynchronization, animals were tested for glucose and insulin tolerance at the end of the ten-week feeding period (Figure 5). While glucose utilization and insulin sensitivity did not depend on SCN clock function in light-dark conditions (Figure 5A; $p = 0.7279$ and 0.7899), in constant darkness glucose tolerance was impaired in SCN-BKO animals compared to control littermates ($p = 0.0252$), while insulin responses stayed roughly comparable between both genotypes ($p = 2117$; Figure 5B). Together, these data suggest that loss of behavioral and/or molecular peripheral clock rhythmicity affects metabolic set points in the absence of a functional SCN clock.

3.3. Time-restricted feeding restores behavioral and molecular clock rhythms and metabolism in SCN-BKO mice in constant darkness

Until ten weeks of age, mice of both genotypes were housed in light-dark and *ad-libitum* chow conditions and then transferred into constant darkness with food access restricted to 12 h per day (from 6:00 in the morning to 18:00 in the evening). Under these time-restricted feeding, but constant darkness conditions (DD-RF), control and SCN-BKO animals retained rhythmic running-wheel activity with a period of 24 h (Figure 6A). However, while control animal activity onsets were located at 4.0 ± 0.6 h before food was provided, the main activity of SCN-BKO mice shifted well into the original light period preceding food access with activity onsets at 8.5 ± 1.1 h before food supply (Suppl. Fig. 3). After one week of restricted feeding conditions, expression of *Bmal1* and *Per2* mRNAs in three metabolic tissues — pancreas, liver, and

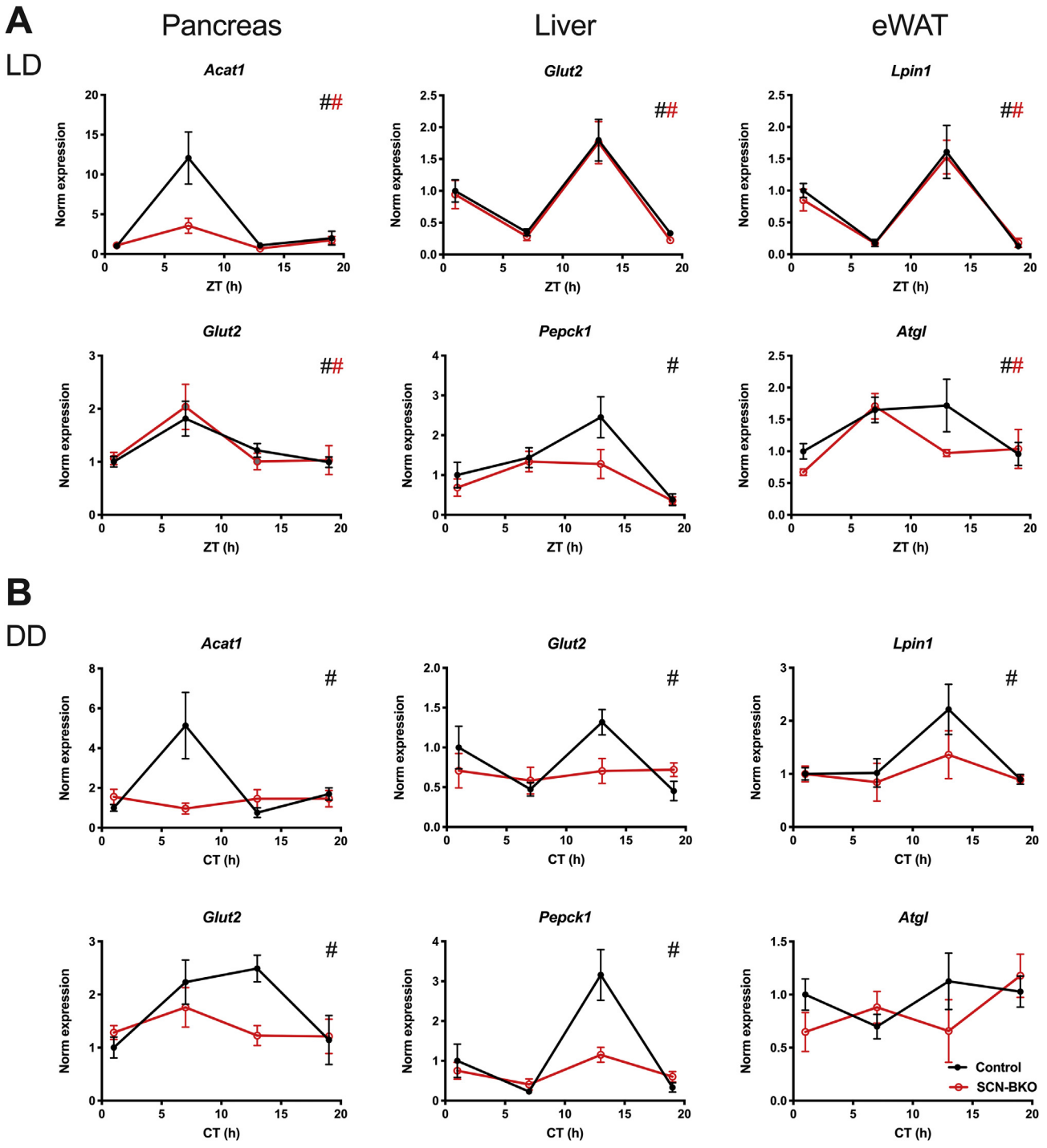

Figure 3: SCN-BKO mice retain metabolic gene rhythms in peripheral tissues under light-dark, but not under constant darkness conditions. A) mRNA expression profiles of *Acat1 (*acetyl-CoA acetyltransferase 1) and *Glut2* (glucose transporter 2; *Slc2a2*) in pancreas, *Glut2* and *Pepck1* (phosphoenolpyruvate carboxykinase) in liver, and *Lpin1* (lipin 1), and *Atgl* (adipose tissue glycerolipase) in eWAT at four time points (*Zeitgeber* time (ZT) 1 = 1 h after "lights on") under light-dark conditions in control and SCN-BKO animals. B) mRNA expression profiles of *Acat1, Glut2* (pancreas), *Glut2, Pepck1* (liver), and *Lpin1, Atgl* (eWAT) at four time points (circadian time (CT) 1 = 37 h after "lights off") under constant darkness conditions in control and SCN-BKO animals (n = 3–5 animals per time point and genotype, #: rhythmic gene expression, $p < 0.05$, CircWave analysis).

eWAT — was assessed at two opposite diurnal time points (7:00 in the morning and 19:00 in the evening). Similar to activity, peripheral clock gene expression rhythms were restored under these conditions, but, unlike activity, the phasing of *Per2* and *Bmal1* rhythms was highly comparable between both genotypes (Figure 6B).

To test if this reintroduction of behavioral and peripheral rhythmicity affects long-term metabolic homeostasis, food intake and body weight regulation were measured for 10 weeks under constant darkness/ restricted feeding conditions. Under these conditions, body weight gain of SCN-BKO mice was normalized to that of control animals (Figure 7A,

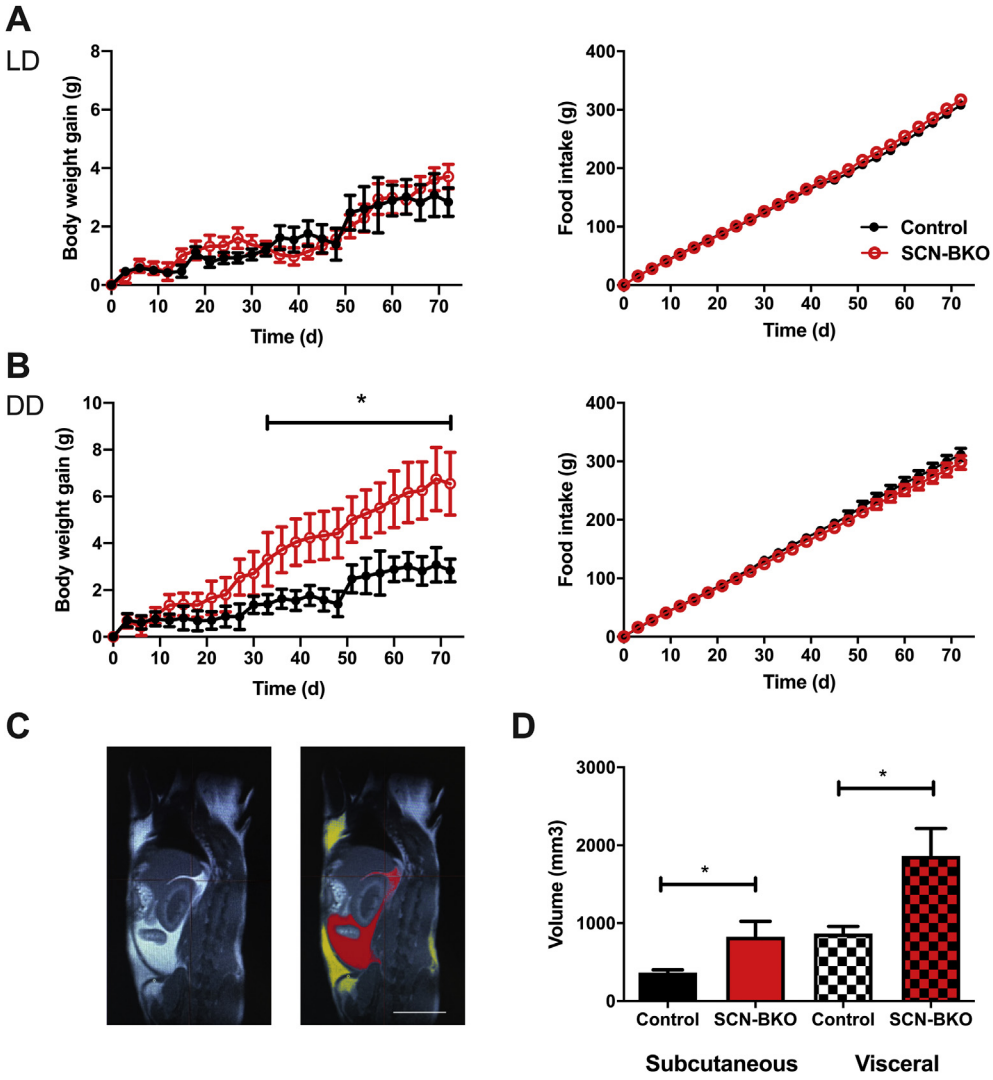

Figure 4: SCN-BKO mice gain fat mass under constant darkness, but not under light-dark conditions. A) Body weight gain (left) and cumulative food intake (right) of control (black) and SCN-BKO (red) mice in light-dark over 10 weeks (weight ANOVA: interaction: $p > 0.999$; time: $p < 0.001$; genotype: $p = 0.478$; food ANOVA: interaction: $p = 0.993$; time: $p < 0.001$; genotype: $p = 0.064$). B) Body weight gain (left) and cumulative food consumption (right) of control (black) and SCN-BKO (red) mice in constant darkness over 10 weeks ($n = 6$ animals per genotype, *: $p < 0.05$, 2-way ANOVA with Bonferroni post-test) (weight ANOVA: interaction: $p < 0.001$; time: $p < 0.001$; genotype: $p = 0.055$; food ANOVA: interaction: $p > 0.999$; time: $p < 0.001$; genotype: $p = 0.002$). C) Body fat distribution analysis. Raw MRI image (left) and marking of visceral (red) and subcutaneous (yellow) adipose tissue (right). White bar corresponds to 100 mm. Evaluation of body fat depot volume of subcutaneous (Sub) and visceral (Vis) adipose tissue in control (black) and SCN-BKO (red) mice after 10 weeks in constant darkness with chow *ad libitum* ($n = 6$ animals per genotype, *: $p < 0.05$, 2-way ANOVA; interaction: $p = 0.214$; depot: $p = 0.002$; genotype: $p = 0.003$).

Table 1 — Metabolic parameters in SCN-BKO and control mice. Daily averages of non-fasted animals; $n = 8–19$; bold type = $p < 0.05$ (unpaired *t*-test).

Metabolic parameter	Light-dark conditions		Constant darkness	
	Control	SCN-BKO	Control	SCN-BKO
Free fatty acids (mMol)	1.7 ± 0.1	1.5 ± 0.2	1.9 ± 0.1	**1.3 ± 0.1**
Glucagon (pMol)	5.8 ± 0.7	5.5 ± 0.4	5.3 ± 0.8	6.0 ± 0.8
Glucose (mg/dl)	127 ± 3	133 ± 4	130 ± 2	**141 ± 5**
Insulin (µg/l)	1.8 ± 0.2	2.5 ± 0.4	1.5 ± 0.2	1.9 ± 0.3
Leptin (µg/l)	2.7 ± 0.6	3.3 ± 0.4	2.2 ± 0.6	**3.6 ± 0.3**
Triglycerides (g/l)	0.98 ± 0.03	0.97 ± 0.03	0.98 ± 0.06	**1.15 ± 0.09**

Bold type signifies $p < 0.05$ (unpaired t-test).

left panel). Interestingly, SCN-BKO animals consumed even slightly less chow over the whole experiment than control mice (Figure 7A, right panel). Like body weight, glucose utilization and insulin sensitivity in SCN-Mut animals were normalized to control levels ($p = 0.5668$ and 0.8154; Figure 7B,C). At the end of the experiment, no further difference was detectable in adiposity and adipose depot distribution ($p = 0.2840$ & 0.2642; Figure 7D, left panel). In direct comparison of all three conditions and genotypes, body weight regulation was stable for control animals while in animals without a functional SCN clock, body weight gain was increased under constant darkness ($p = 0.0303$), but not constant darkness/restricted feeding conditions ($p = 0.6955$), suggesting that restoration of behavioral/molecular rhythms can compensate for the loss of a functional pacemaker in SCN-BKO mice.

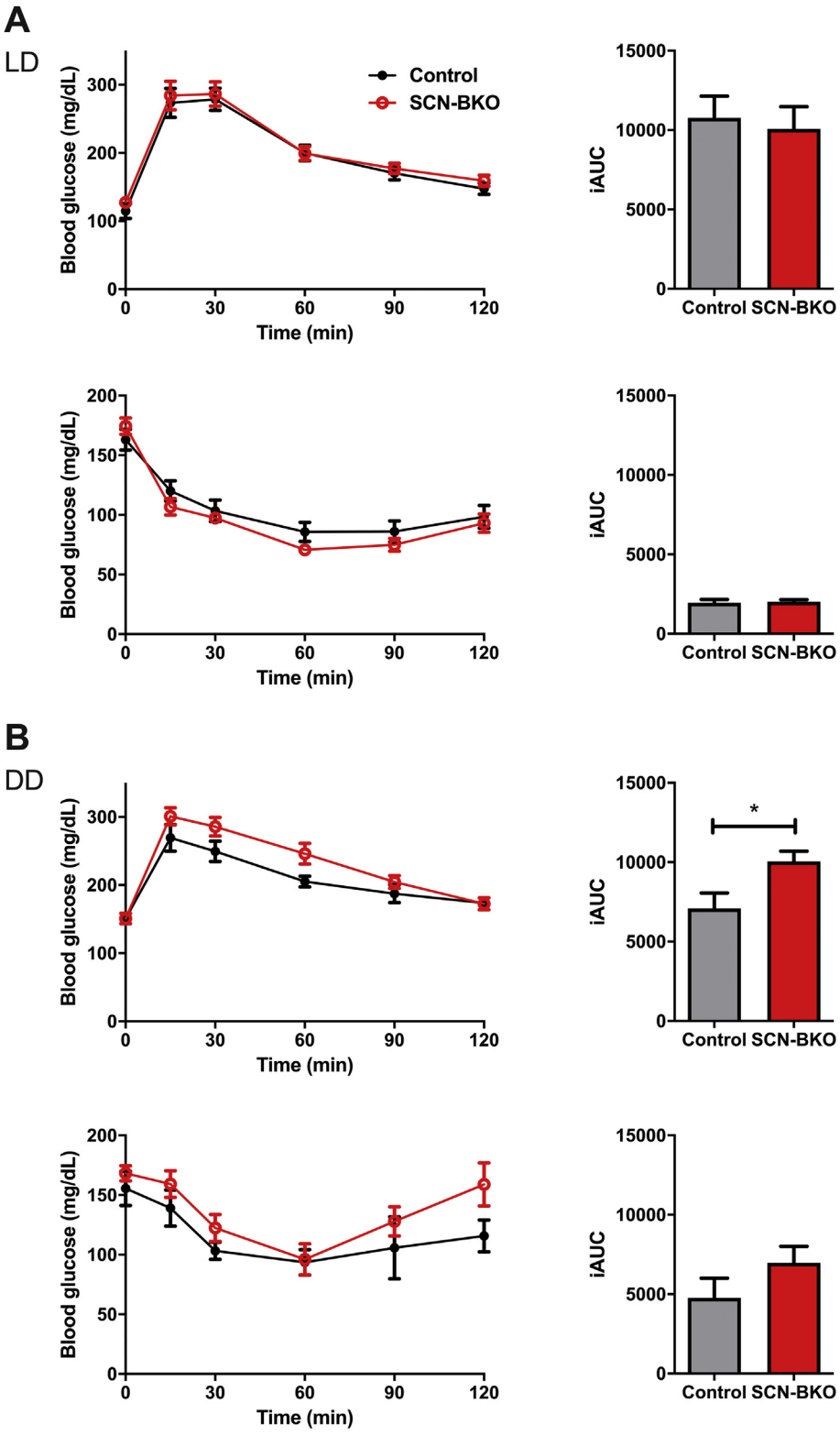

Figure 5: Impaired glucose utilization in SCN-BKO mice in constant darkness. A) Intraperitoneal glucose (upper panel) and insulin (lower panel) tolerance tests in control (black) and SCN-BKO (red) animals with the corresponding incremental area under the curve (iAUC) evaluation on the right in light-dark (glucose ANOVA: interaction: $p = 0.992$; time: $p < 0.001$; genotype: $p = 0.530$; insulin ANOVA: interaction: $p = 0.341$; time: $p < 0.001$; genotype: $p = 0.367$)) and B) in DD (glucose ANOVA: interaction: $p = 0.090$; time: $p < 0.001$; genotype: $p = 0.111$; insulin ANOVA: interaction: $p = 0.741$; time: $p < 0.001$; genotype: $p = 0.112$) ($n = 6$ animals per genotype; iAUC: *: $p < 0.05$, unpaired Student's t-test).

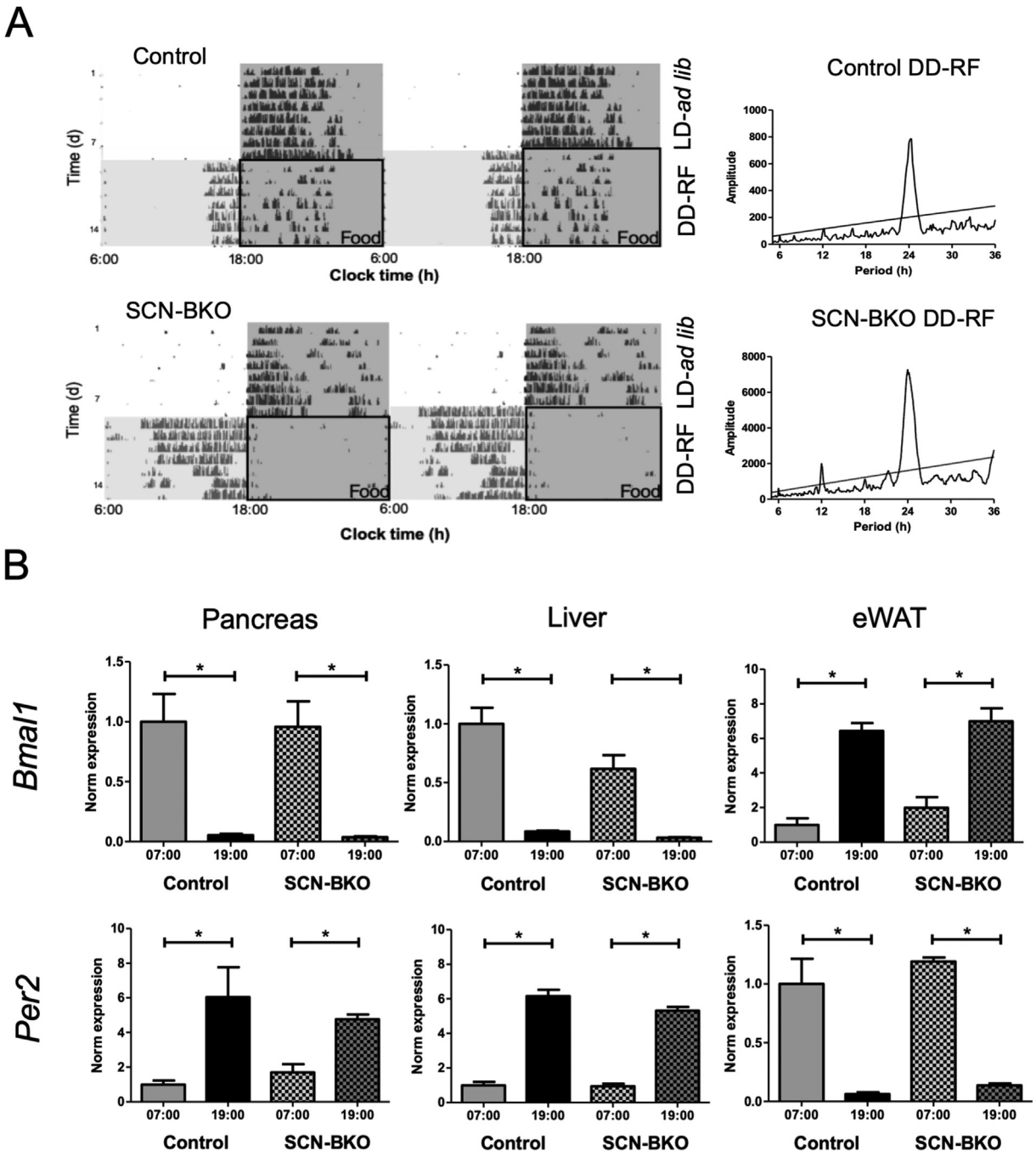

Figure 6: Time restricted feeding (RF) restores rhythmic behavior and peripheral clock synchrony in SCN-BKO mice in constant darkness. A) Representative actograms (left) of control (upper panel) and SCN-BKO (lower panel) mice in light-dark with *ad-libitum* food access followed by constant darkness and time restricted feeding conditions (DD-RF). Food-in phases under RF are indicated by black boxes. Grey shading signifies dark phases. Right: corresponding $\chi 2$ periodograms for the restricted feeding conditions for both genotypes. B) mRNA expression of *Bmal1* and *Per2* under restricted feeding conditions in control and SCN-BKO animals in pancreas (*Bmal1* ANOVA: interaction: $p = 0.938$; time: $p < 0.001$; genotype: $p = 0.857$; *Per2* ANOVA: interaction: $p = 0.309$; time: $p = 0.002$; genotype: $p = 0.758$), liver (*Bmal1* ANOVA: interaction: $p = 0.103$; time: $p < 0.001$; genotype: $p = 0.042$; *Per2* ANOVA: interaction: $p = 0.148$; time: $p < 0.001$; genotype: $p = 0.104$) and epididymal white adipose tissue (*Bmal1* ANOVA: interaction: $p = 0.588$; time: $p < 0.001$; genotype: $p = 0.249$; *Per2* ANOVA: interaction: $p = 0.610$; time: $p < 0.001$; genotype: $p = 0.147$) one hour after food removal (7:00) and one hour after food access (19:00; $n = 3$ animals per time point and genotype, *: $p < 0.05$, 2-way ANOVA with Bonferroni post-test).

4. DISCUSSION

Circadian rhythms are important regulators of metabolic health. They are the output of a coordinative network of cellular oscillators. In this study, we addressed the question of the importance of peripheral network synchronization for metabolic homeostasis in male mice. We found that under rhythmic environmental conditions — light or food access — the synchronizing SCN pacemaker function is dispensable for normal metabolic regulation while in constant darkness the SCN becomes a critical factor in the maintenance of systemic synchrony for

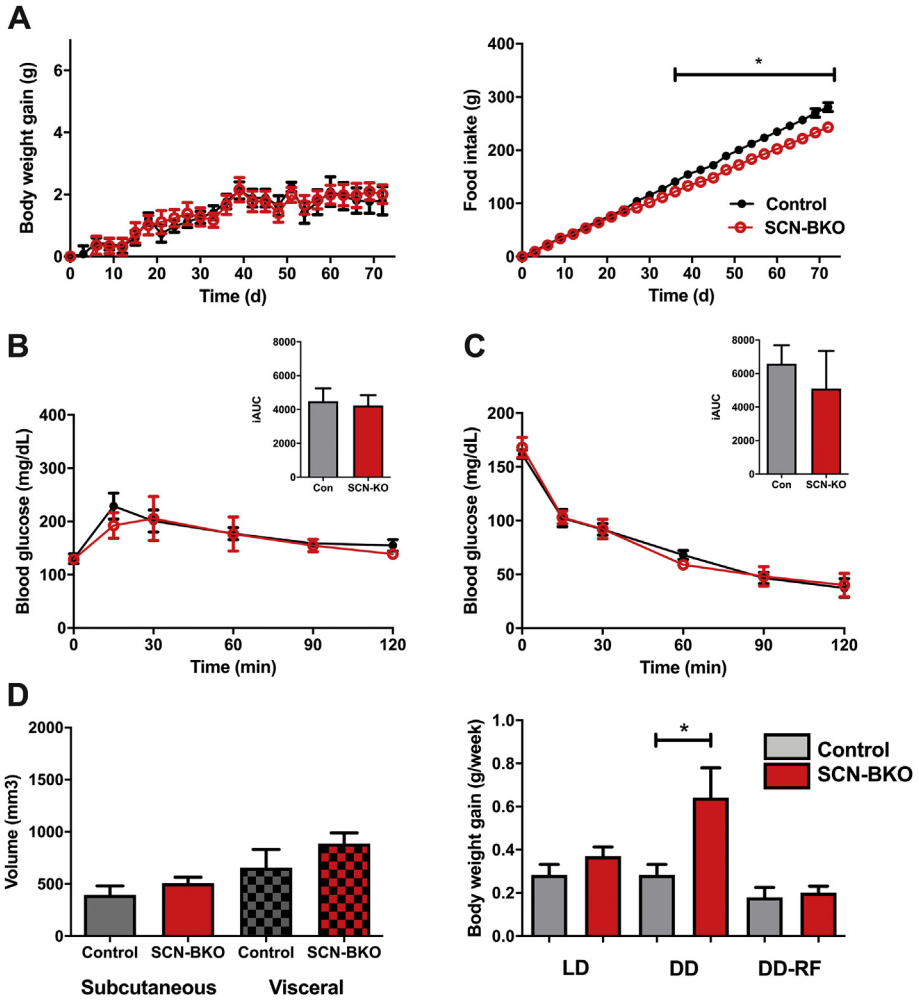

Figure 7: Restricted feeding reduces food intake in SCN-BKO animals and normalizes glucose response, body weight, and body composition. A) Body weight gain (left) and cumulative food intake (right) of control (black) and SCN-BKO (red) mice in restricted feeding conditions over 10 weeks (weight ANOVA: interaction: $p = 0.492$; time: $p < 0.001$; genotype: $p = 0.697$; food ANOVA: interaction: $p < 0.001$; time: $p < 0.001$; genotype: $p = 0.004$). B) Intraperitoneal glucose (ANOVA: interaction: $p = 0.801$; time: $p < 0.001$; genotype: $p = 0.671$) and C) insulin tolerance tests (ANOVA: interaction: $p = 0.884$; time: $p < 0.001$; genotype: $p = 0.928$) under restricted feeding conditions in control (black) and SCN-BKO (red) animals with the corresponding incremental area under the curve (iAUC) evaluations on the right ($n = 6$ animals per genotype, iAUC: Student's t-test) D) Body fat depot volume (left) of subcutaneous and visceral adipose tissue in control (grey) and SCN-BKO (red) mice after 10 weeks in restricted feeding (ANOVA: interaction: $p = 0.597$; depot: $p < 0.009$; genotype: $p = 0.132$). Body weight gain per week of control and SCN-BKO animals in light-dark and constant darkness *ad libitum* and restricted feeding conditions (right; $n = 6$ animals per genotype, *: $p < 0.05$, 2-way ANOVA with Bonferroni post-test).

normal body weight and glucose tolerance. These data support an organized model of the circadian clock network and highlight the importance of peripheral tissue clock coordination in metabolic health. Circadian rhythms and energy homeostasis are deeply linked as suggested by epidemiological studies on shift workers but also human forced desynchrony laboratory studies and animal data, e.g. on clock gene mutant mice [10,15]. SCN surgical lesions or exposure of animals to SCN clock-disrupting constant light conditions promote body weight gain and insulin resistance suggesting an essential role of the SCN pacemaker in metabolic homeostasis [16,24]. On the other hand, conditional deletion of clock function in several peripheral tissues such as liver, muscle, adipose tissue, or pancreatic beta cells has been shown to critically affect energy metabolic homeostasis [7,8,12,18,19]. Moreover, we have recently shown that liver clock gene therapy can restore body weight regulation under high-fat diet conditions in *Clock* gene mutant mice [17]. Together these data suggest that circadian network coordination — including central as well as peripheral tissue clocks — is crucial for metabolic health. Our findings support this idea showing that under rhythmic environmental conditions — light-dark or time restricted feeding, which reset behavior and peripheral tissue clocks — SCN pacemaker function is dispensable for normal metabolic regulation.

When reinstating rhythmic feeding behavior by time-restricted food access in constant darkness, metabolic regulation in SCN-BKO mice became restored. Such an important role of behavioral rhythmicity in metabolic regulation has been demonstrated in a row of studies on time-restricted feeding by the Panda lab showing that night-time restricted food access largely neutralizes the obesogenic effect of a high-fat diet [25] and can even compensate for genetic disruptions of the circadian clock system [26]. We show that under restricted feeding conditions peripheral clock gene rhythms were restored in SCN-BKO mice despite a non-functional SCN clock. This is in line with previous transcriptomics data showing a dominant function of feeding behavior on gene expression rhythms in metabolic tissues such as the liver [2]. Interestingly — and unlike most SCN-lesioned animals [27] — mice with a genetically ablated SCN clock display intact light masking

behavior and therefore stay behaviorally rhythmic in light-dark conditions [22,28]. In parallel to locomotor activity, food intake in SCN-BKO mice was rhythmic in light-dark conditions with most food being consumed during the active hours in the dark phase and the functional peripheral clocks stay aligned. Temperature rhythms in light-dark can also be a direct result of the still rhythmic food intake as in light-dark SCN-lesioned mice do not display rhythmic body temperature [16], but, in intact SCN animals, restricted feeding can uncouple temperature oscillations from the SCN [29]. Under such light-masked conditions, rhythmic behavior in SCN-BKO mice is a direct result of light exposure as the non-functional SCN clock cannot be entrained, but rhythmic light input can pass the SCN to reach downstream tissues to synchronize functional tissue clocks and drive systemic circadian signals such as glucocorticoid release, rest/activity behavior, or food intake [22]. In the absence of external light, the lack of synchronizing signals from a functional SCN becomes a liability resulting in loss of rhythmicity in running-wheel behavior, food intake, and endocrine rhythms, resembling what is observed already under light-dark conditions in SCN-lesioned animals [16].

SCN-BKO mice gained more weight than control animals in constant darkness despite comparable food intake. This may reflect the non-rhythmic distribution of feeding episodes across the circadian day. Previous studies have shown that increased food intake during the normal resting phase causes weight gain despite comparable caloric intake [30]. Also in constant darkness, adipogenesis is increased, which is also seen in mice with adipose clock impairments in which the diurnal lipid mobilization from adipose tissue is inhibited [31–34]. As a consequence, the concentration of fatty acids in the blood is reduced, and the organism mainly utilizes carbohydrates for energy demands [35]. The preference for a carbohydrate-driven metabolism in clock mutants and in SCN-BKO can be a hallmark for an impaired metabolic flexibility [36] and a suppressed lipid mobilization may promote weight gain due to increased triglyceride storage in adipose tissues [34] as triglycerides are synthesized during the time of energy surplus and stored, but not utilized in times of energy demand. In line with this, the circadian regulation of transcripts encoding for regulators of glucose and lipid metabolism was altered in SCN-BKO mice in constant darkness, suggesting that a loss of peripheral clock synchrony may lead to alterations in energy conversion, ultimately resulting in adverse effects on energy homeostasis (Suppl. Figure 4). In contrast to the results obtained in light-dark conditions, where glucose metabolism was unaltered, glucose clearance was decreased in SCN-BKOs in constant darkness conditions while sensitivity to insulin was comparable in both conditions, indicating that tissues are still insulin sensitive, but pancreatic insulin release in response to glucose administration [37] may be impaired. However, differences were modest and overall insulin responses were subtle, probably due to the short fasting and normal chow conditions. This may be a possible result of peripheral desynchronization and the loss of a clock gated pancreatic insulin release [38]. Restricted access to food could have restored glucose sensitivity in SCN-BKO animals and influence metabolic outcome, as clocks in beta-cells are sensitive to food resetting [37]. Restricted food access stabilizes blood insulin and glucose clearance under chow and rescues glucose homeostasis under high-fat diet feeding in wild type and also in clock deficient mice [25,26]. While the master SCN clock stays mainly aligned to the light dark cycle, peripheral oscillators are sensitive to the timing of food intake and can be completely uncoupled from the master clock [39]. In the case of a non-functional SCN clock and missing light cues, restricted feeding takes over as a main *zeitgeber* realigning the peripheral clock network [40]. Time restricted feeding stabilizes the clock gene expression in liver in chow-fed conditions and recues the weight and glucose homeostasis in high-fat diet challenged animals [25]. Restricted feeding also restored 24-hour activity rhythms in SCN-BKO mice, albeit at a strongly altered phase and reduced overall levels. Of note, even in light-dark conditions, restricted feeding can trigger anticipatory activity for several hours, and a strong shift in activity was observed in mice with a genetically deleted SCN clock function [28]. To which extent this differential shift in locomotor activity contributes to the restoration of energy metabolism and which tissue clocks may be involved in this phenomenon remain to be shown.

In conclusion, we show that a functional SCN clock is not needed to sustain metabolic health in a rhythmic environment, which is sufficient to drive behavioral and peripheral clock network rhythms. In constant conditions, however, the synchronizing capacity of the master clock becomes key for this synchronization and metabolic homeostasis. These data recalibrate the roles of the SCN pacemaker and peripheral clocks in the coordination of physiology and argue towards a federated model of circadian timekeeping and circadian physiology.

ACKNOWLEDGEMENTS

This work was supported by grants of the German Research Foundation (DFG; GRK 1957 and OS353/7-1). HO is a Lichtenberg fellow of the Volkswagen Foundation.

CONFLICT OF INTEREST

None declared.

APPENDIX A. SUPPLEMENTARY DATA

Supplementary data to this article can be found online at https://doi.org/10.1016/j.molmet.2019.09.012.

REFERENCES

[1] Buhr, E.D., Takahashi, J.S., 2013. Molecular components of the Mammalian circadian clock. Handbook of Experimental Pharmacology 217:3–27.

[2] Vollmers, C., Gill, S., DiTacchio, L., Pulivarthy, S.R., Le, H.D., Panda, S., 2009 Dec. Time of feeding and the intrinsic circadian clock drive rhythms in hepatic gene expression. Proceedings of the National Academy of Sciences of the United States of America 106(50):21453–21458.

[3] Golombek, D.A., Rosenstein, R.E., 2010 Jul. Physiology of circadian entrainment. Physiological Reviews 90(3):1063–1102.

[4] Ángeles-Castellanos, M., Amaya, J.M., Salgado-Delgado, R., Buijs, R.M., Escobar, C., 2011 Aug. Scheduled food hastens re-entrainment more than melatonin does after a 6-h phase advance of the light-dark cycle in rats. Journal of Biological Rhythms 26(4):324–334.

[5] Laemle, L.K., Ottenweller, J.E., 1999 May. Nonphotic entrainment of activity and temperature rhythms in anophthalmic mice. Physiology & Behavior 66(3):461–471.

[6] Sukumaran, S., Xue, B., Jusko, W.J., DuBois, D.C., Almon, R.R., 2010 Oct. Circadian variations in gene expression in rat abdominal adipose tissue and relationship to physiology. Physiological Genomics 42A(2):141–152.

[7] Sadacca, L.A., Lamia, K.A., deLemos, A.S., Blum, B., Weitz, C.J., 2011 Jan. An intrinsic circadian clock of the pancreas is required for normal insulin release and glucose homeostasis in mice. Diabetologia 54(1):120–124.

[8] Marcheva, B., Ramsey, K.M., Buhr, E.D., Kobayashi, Y., Su, H., Ko, C.H., et al., 2010 Jul. Disruption of the clock components CLOCK and BMAL1 leads to hypoinsulinaemia and diabetes. Nature 466(7306):627–631.

[9] Grant, C.L., Coates, A.M., Dorrian, J., Kennaway, D.J., Wittert, G.A., Heilbronn, L.K., et al., 2017. Timing of food intake during simulated night shift impacts glucose metabolism: a controlled study. Chronobiology International 34(8):1003–1013.

[10] Scheer, F.A.J.L., Hilton, M.F., Mantzoros, C.S., Shea, S.A., 2009 Mar. Adverse metabolic and cardiovascular consequences of circadian misalignment. Proceedings of the National Academy of Sciences of the United States of America 106(11):4453–4458.

[11] Hemmers, S., Rudensky, A.Y., 2015 Jun. The cell-intrinsic circadian clock is dispensable for lymphocyte differentiation and function. Cell Reports 11(9): 1339–1349.

[12] Lamia, K.A., Storch, K.-F., Weitz, C.J., 2008 Sep. Physiological significance of a peripheral tissue circadian clock. Proceedings of the National Academy of Sciences of the United States of America 105(39):15172–15177.

[13] Rudic, R.D., McNamara, P., Curtis, A.M., Boston, R.C., Panda, S., Hogenesch, J.B., et al., 2004 Nov. BMAL1 and CLOCK, two essential components of the circadian clock, are involved in glucose homeostasis. PLoS Biology 2(11):e377.

[14] Shimba, S., Ogawa, T., Hitosugi, S., Ichihashi, Y., Nakadaira, Y., Kobayashi, M., et al., 2011. Deficient of a clock gene, brain and muscle Arnt-like protein-1 (BMAL1), induces dyslipidemia and ectopic fat formation. PLoS One 6(9):e25231.

[15] Turek, F.W., Joshu, C., Kohsaka, A., Lin, E., Ivanova, G., McDearmon, E., et al., 2005 May. Obesity and metabolic syndrome in circadian Clock mutant mice. Science 308(5724):1043–1045.

[16] Coomans, C.P., van den Berg, S.A., Lucassen, E.A., Houben, T., Pronk, A.C., van der Spek, R.D., et al., 2013 Apr. The suprachiasmatic nucleus controls circadian energy metabolism and hepatic insulin sensitivity. Diabetes 62(4): 1102–1108.

[17] Meyer-Kovac, J., Kolbe, I., Ehrhardt, L., Leliavski, A., Husse, J., Salinas, G., et al., 2017 Jun. Hepatic gene therapy rescues high-fat diet responses in circadian Clock mutant mice. Molecular Metabolism 6(6):512–523.

[18] Dyar, K.A., Ciciliot, S., Wright, L.E., Biensø, R.S., Tagliazucchi, G.M., Patel, V.R., et al., 2014 Feb. Muscle insulin sensitivity and glucose metabolism are controlled by the intrinsic muscle clock. Molecular Metabolism 3(1):29–41.

[19] Paschos, G.K., Ibrahim, S., Song, W.L., Kunieda, T., Grant, G., Reyes, T.M., et al., 2012 Dec. Obesity in mice with adipocyte-specific deletion of clock component Arntl. Nature Medicine 18(12):1768–1777.

[20] Husse, J., Eichele, G., Oster, H., 2015 Oct. "Synchronization of the mammalian circadian timing system: light can control peripheral clocks independently of the SCN clock: alternate routes of entrainment optimize the alignment of the body's circadian clock network with external time. BioEssays News and Reviews in Molecular, Cellular and Developmental Biology 37(10):1119–1128.

[21] Husse, J., Zhou, X., Shostak, A., Oster, H., Eichele, G., 2011 Oct. Synaptotagmin10-Cre, a driver to disrupt clock genes in the SCN. Journal of Biological Rhythms 26(5):379–389.

[22] Husse, J., Leliavski, A., Tsang, A.H., Oster, H., Eichele, G., 2014 Nov. The light-dark cycle controls peripheral rhythmicity in mice with a genetically ablated suprachiasmatic nucleus clock. FASEB Journal Of Publication Federation of American Societes of Experimental Biology 28(11):4950–4960.

[23] Zhang, R., Lahens, N.F., Ballance, H.I., Hughes, M.E., Hogenesch, J.B., 2014 Nov. A circadian gene expression atlas in mammals: implications for biology and medicine. Proceedings of the National Academy of Sciences of the United States of America 111(45):16219–16224.

[24] Coomans, C.P., van den Berg, S.A., Houben, T., van Klinken, J.B., van den Berg, R., Pronk, A.C., et al., 2013 Apr. Detrimental effects of constant light exposure and high-fat diet on circadian energy metabolism and insulin sensitivity. FASEB Journal Of Publication Federation of American Societes of Experimental Biology 27(4):1721–1732.

[25] Hatori, M., Vollmers, C., Zarrinpar, A., DiTacchio, L., Bushong, E.A., Gill, S., et al., 2012 Jun. Time-restricted feeding without reducing caloric intake prevents metabolic diseases in mice fed a high-fat diet. Cell Metabolism 15(6):848–860.

[26] Chaix, A., Lin, T., Le, H.D., Chang, M.W., Panda, S., 2019 Feb 5. Time-restricted feeding prevents obesity and metabolic syndrome in mice lacking a circadian clock. Cell Metabolism 29(2):303–319.

[27] Stephan, F.K., Zucker, I., 1972 Jun. Circadian rhythms in drinking behavior and locomotor activity of rats are eliminated by hypothalamic lesions. Proceedings of the National Academy of Sciences of the United States of America 69(6):1583–1586.

[28] Izumo, M., Pejchal, M., Schook, A.C., Lange, R.P., Walisser, J.A., Sato, T.R., et al., 2014 Dec. Differential effects of light and feeding on circadian organization of peripheral clocks in a forebrain Bmal1 mutant. eLife 3.

[29] Sen, S., Raingard, H., Dumont, S., Kalsbeek, A., Vuillez, P., Challet, E., 2017. Ultradian feeding in mice not only affects the peripheral clock in the liver, but also the master clock in the brain. Chronobiology International 34(1):17–36.

[30] Arble, D.M., Bass, J., Laposky, A.D., Vitaterna, M.H., Turek, F.W., 2009 Nov. Circadian timing of food intake contributes to weight gain. Obesity Silver Spring Md 17(11):2100–2102.

[31] Guo, B., Chatterjee, S., Li, L., Kim, J.M., Lee, J., Yechoor, V.K., et al., 2012 Aug. The clock gene, brain and muscle Arnt-like 1, regulates adipogenesis via Wnt signaling pathway. FASEB Journal Of Publication Federation of American Societes of Experimental Biology 26(8):3453–3463.

[32] Kennaway, D.J., Owens, J.A., Voultsios, A., Boden, M.J., Varcoe, T.J., 2007 Oct. Metabolic homeostasis in mice with disrupted Clock gene expression in peripheral tissues. American Journal of Physiology - Regulatory, Integrative and Comparative Physiology 293(4):R1528–R1537.

[33] Oishi, K., Atsumi, G., Sugiyama, S., Kodomari, I., Kasamatsu, M., Machida, K., et al., 2006 Jan. Disrupted fat absorption attenuates obesity induced by a high-fat diet in Clock mutant mice. FEBS Letters 580(1):127–130.

[34] Shostak, A., Meyer-Kovac, J., Oster, H., 2013 Jul. Circadian regulation of lipid mobilization in white adipose tissues. Diabetes 62(7):2195–2203.

[35] Wu, J.W., Wang, S.P., Casavant, S., Moreau, A., Yang, G.S., Mitchell, G.A., May 2012. Fasting energy homeostasis in mice with adipose deficiency of desnutrin/adipose triglyceride lipase. Endocrinology 153(5):2198–2207.

[36] Kelley, D.E., He, J., Menshikova, E.V., Ritov, V.B., 2002 Oct. Dysfunction of mitochondria in human skeletal muscle in type 2 diabetes. Diabetes 51(10): 2944–2950.

[37] Rakshit, K., Qian, J., Colwell, C.S., Matveyenko, A.V., 2015 Sep. The islet circadian clock: entrainment mechanisms, function and role in glucose homeostasis. Diabetes, Obesity and Metabolism 17(Suppl 1):115–122.

[38] Perelis, M., Ramsey, K.M., Bass, J., 2015 Sep. The molecular clock as a metabolic rheostat. Diabetes, Obesity and Metabolism 17(Suppl 1):99–105.

[39] Damiola, F., Le Minh, N., Preitner, N., Kornmann, B., Fleury-Olela, F., Schibler, U., 2000 Dec. Restricted feeding uncouples circadian oscillators in peripheral tissues from the central pacemaker in the suprachiasmatic nucleus. Genes & Development 14(23):2950–2961.

[40] Saini, C., Suter, D.M., Liani, A., Gos, P., Schibler, U., 2011. The mammalian circadian timing system: synchronization of peripheral clocks. Cold Spring Harbor Symposia on Quantitative Biology 76:39–47.

